Műszaki Tudományos Közlemények vol. 10. (2019) 49–54.
https://doi.org/10.33894/mtk-2019.10.06
Hungarian: https://doi.org/10.33865/mtk-2019.10.06,
https://eda.eme.ro/handle/10598/31165

THE NUMERICAL EVALUATION ERRORS OF THE GEOMETRIC MODEL OF THE STRAIGHT TEETHED SHAPER CUTTER

Márton MÁTÉ,[1] Dénes HOLLANDA [2]

Sapientia Hungarian University of Transylvania, Târgu-Mureș, Faculty of Technical and Human Sciences, Department of Mechanical Engineering, Târgu-Mureș, Romania

[1] *mmate@ms.sapientia.ro*

[2] *hollanda@ms.sapientia.ro*

Abstract

It is well known that straight teethed shaper cutters present a theoretical profile error. The side edges are situated on a common conical rack face with the result that they and their projection in the generating plane can't be involute curves. The optimization of the cutter requires such a correlation of the edge defining parameters that the potential theoretical profile error is kept to the minimum possible. Thus the relevance of the edge equations is of great importance. This paper deals with the analysis of the edge equations, presenting two different forms of it. The comparison between the two different forms is realized by applying the numerical evaluation, by substitution of the edge point coordinates in the implicit equations of the originating surfaces. The obtained results present a difference of magnitude 10-E3. Finally, it can be concluded that the two forms of the edge equations cannot be used randomly but only in correlation with the goal proposed by the running application.

Keywords*: shaper cutter, model, edge, profile error, computing error.*

1. The geometric model of the straight teethed shaper cutter

The geometric model of the straight teethed shaper cutter is based on the theory of classical meshing with a rack **[1, 2, 3, 4]**. The rack profile is rectilinear. Its profile angle is denoted with α_{0S} that differs from those of the gear generating rack. During the meshing process the rack produces a linearly descending specific profile shift starting from the basic plane in the height of the cutter. As a consequence of this particularity, the tooth flanks result as helical involute surfaces having opposite senses. The topland surface is a circular cone defined by the half-angle α_V and the addendum circle with radius R_a. The pitch helix angle β_0 of the flanks can be deduced using simple geometric relations **[3, 4]**

$$\operatorname{tg}\beta_0 = \operatorname{tg}\alpha_V \operatorname{tg}\alpha_{0s} \tag{1}$$

The basic helix angle value results from the dependence between the pitch and basic radii:

$$\operatorname{tg}\beta_b = \operatorname{tg}\alpha_V \sin\alpha_{0s} \tag{2}$$

Using as input values the teeth number z_s, the specific profile shift and the module m, the second basic equation of the involute trigonometry **[5]** allows us to compute the angle η between the involute basic point radius and the symmetry axis $O_s x_s$ of the tooth profile (**Figure 1**):

$$\eta = \frac{\pi}{2z_s} + 2\frac{\xi_s}{z_s}\operatorname{tg}\alpha_{0s} + \operatorname{inv}\alpha_{0s} \tag{3}$$

1.1. The tooth flank- the side relief face

The equations of the tooth flank are deduced by virtue of **Figure 1.** The manufacturing of involute helix surfaces can be realized using several technologies **[4, 6, 7, 8]**, but the kinematic geometry offers only the following two possibilities:

– applying a helical transformation to the involute arch situated in the basic plane, or
– meshing it by a straight line, included in a plane [S], closing the angle β_b with the axis of the basic cylinder, while the plane rolls on this.

Considering the first method, and using the notations shown on **Figure 1.** the equations of the involute (considered also the generating curve) result in the form shown below **[9]**:

$$\begin{cases} x(u) = R_b\left(\cos(u-\eta) + u\sin(u-\eta)\right) \\ y(u) = R_b\left(\sin(u-\eta) - u\cos(u-\eta)\right) \end{cases} \quad (4)$$

Applying to these a helical transformation along axis Oz_s, value p_w and helix parameter $p = R_0 / \cos\beta_0 = R_b \cos\beta_b$, the following equations are achieved **[9]**:

$$\begin{cases} x_s(u,w) = R_b\left(\cos(u-\eta+w) + u\sin(u-\eta+w)\right) \\ y_s(u,w) = R_b\left(\sin(u-\eta+w) - u\cos(u-\eta+w)\right) \\ z_s(u,w) = pw \end{cases} \quad (5)$$

Figure 1. let us to write the following vectorial equation too:

$$\begin{aligned} &\mathbf{O_sM} = \mathbf{O_sP} + \mathbf{PQ} + \mathbf{QM} \\ &PQ = p\varphi \\ &QM = \lambda \end{aligned} \quad (6)$$

Rewriting this in matrix form, results in:

$$\begin{pmatrix} x_s \\ y_s \\ z_s \end{pmatrix} = \begin{pmatrix} R_b\cos(\varphi-\eta) \\ R_b\sin(\varphi-\eta) \\ 0 \end{pmatrix} + \begin{pmatrix} 0 \\ 0 \\ p\varphi \end{pmatrix} + \begin{pmatrix} \lambda\sin\beta_b\sin(\varphi-\eta) \\ -\lambda\sin\beta_b\cos(\varphi-\eta) \\ -\lambda\cos\beta_b \end{pmatrix} \quad (7)$$

If substituting here parameter λ using the $v = \lambda\sin\beta_b / R_b$ linear transformation the equations (7) become the following shape

$$\begin{cases} x_s(\varphi,v) = R_b\left(\cos(\varphi-\eta) + v\sin(\varphi-\eta)\right) \\ y_s(\varphi,v) = R_b\left(\sin(\varphi-\eta) - v\cos(\varphi-\eta)\right) \\ z_s(\varphi,v) = p(\varphi-v) \end{cases} \quad (8)$$

Comparing equations (5) and (8) the following dependences between the surface parameters can be concluded:

$$\begin{aligned} &\varphi - \eta = u - \eta + w \\ &w = \varphi - v \end{aligned} \quad (9)$$

The geometric meanings of the parameters used in the two different equations are different. Parameter u of equations (5) measures the center angle that corresponds to the arch of run of the involute generating line on the basic circle. Parameter w signifies the rotation part of the helical motion, applied to the developed involute arch length. Both parameter are angles in a geometric sense. Dissimilar to this, angle φ from equations (9) marks the run of the generating line-carrying plane S. Finally, parameter v is a-dimensional

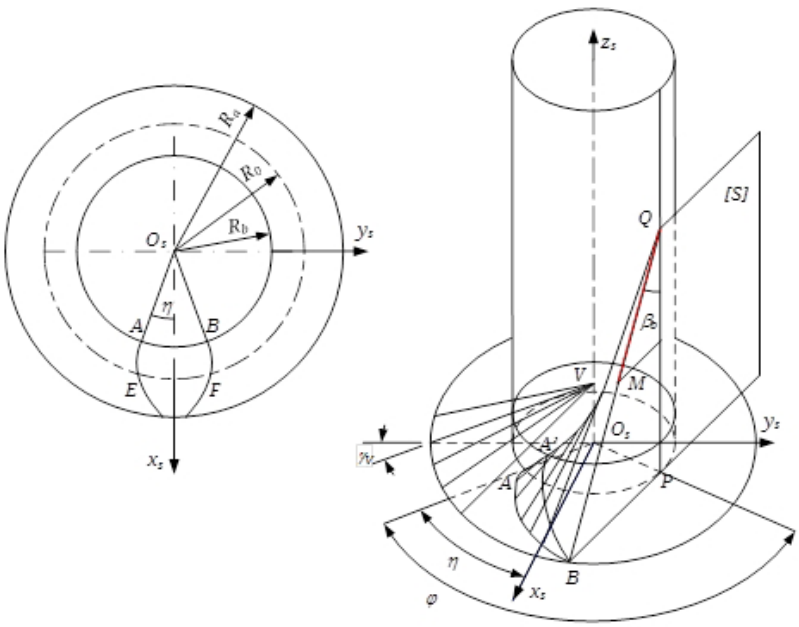

Figure 1. *The geometrical dependences encountered by the meshing of an involute helix surface*

because it primes the quotient of two segments: the first is the projection on the plane *xy* of the generating line part starting from point *Q* and the second is the basic circle radius.

Computing the angle φ from equalities (9) results in

$$w + v = w + u \Leftrightarrow v = u \tag{10}$$

The equality above can induce an error when choosing the interval of variation for the independent surface parameters. Parameter u in equations (5) limits only the length of the involute arch in plane *xy* while parameter v in equations (8) determines the length of the involute arch and in the same time its height over plane *xy*.

In both cases the directory line is the β_b inclination angle characterized helix drawn on the basic cylinder. However the generating lines differ from each other. In the first case this is the involute arch limited between the basic and the addendum circles, in the plane *xy*.

In the second case it is a straight line included in a plane *S* tangent to the basic cylinder and including with these axes the angle β_b.

The parametric form facilitates the generation of the surface's point-cloud. Here the most uniform density is of crucial importance [10]. In the first case this can be achieved by dividing the involute arch into segments of equal length together with the uniform segmentation of the helix motion parameter *w*. It is well known that if the involute drawing line's rolling parameter is linearly increased, the drawn arch segment lengths result in a geometric progression. [5]. in order to avoid this, a nonlinear parameter variation must be applied. From equations (4) the infinitesimal involute arch length is:

$$\mathrm{d}\, s = R_b u\, \mathrm{d}\, u \tag{11}$$

The arch-length corresponding to the arbitrary interval $[u_1,u_2]$, can be computed with the next formula:

$$s_{i,i+1} = \int_{u_i}^{u_{i+1}} \mathrm{d}\, s = \frac{1}{2} R_b \left(u_{i+1}^2 - u_i^2 \right) \tag{12}$$

Thus the length of the involute arch limited by the basic and dedendum circles results as:

$$L = \tfrac{1}{2}\sqrt{R_a^2 - R_b^2} \quad , \tag{13}$$

namely the moiety of the rolled segment length.

A division of *N* points generates *N-1* arch segments whose length is (Figure 1.)

$$\Delta L = L/(N-1) \tag{14}$$

The recursive function between two consequent u parameter values results from (12) where the length of the arch segment is given by (14):

$$u_{i+1} = \sqrt{\frac{2\Delta L}{R_b} + u_i^2} \tag{15}$$

In the second case the values of both parameters must fulfill a non-uniform repartition along their definition interval. This leads to very complicated functions, of little practical use.

From a mathematical point of view equations (8) present a more advantageous form in comparison with form (5) due to the fact that here independent surface parameters φ and v are separated. Thus the expression of the edge function is explicit.

1.2. The rake face

The rake face equations (Figure 2.) can be primed in two different manners:

– using the concurrent lines starting from top *V*;

– using the family of circles parallel with plane *xy*.

The beam starts from top *V(0, 0, h_0)*.

Let u be the distance on the cone generatrix from top *V* to the arbitrary point *M*, while υ denotes the angle between axis *x* and the projection of the generatrix in the plane *xy*. In this situation the parametric equations of the cone are :

$$\begin{aligned} x_s(u,\upsilon) &= u\cos\gamma_V \cos\upsilon \\ y_s(u,\upsilon) &= u\cos\gamma_V \sin\upsilon \\ z_s(u,\upsilon) &= R_a \operatorname{tg}\gamma_v - u\sin\gamma_V + \delta_H \end{aligned} \tag{16}$$

When a re-sharpening of the cutter occurs, the rake face translates along axis *z* in its positive sense with a distance δ_H.

If the conical surfaces are considered as a family of circles situated in parallel planes, the independent parameters are the radius ρ of an arbitrary

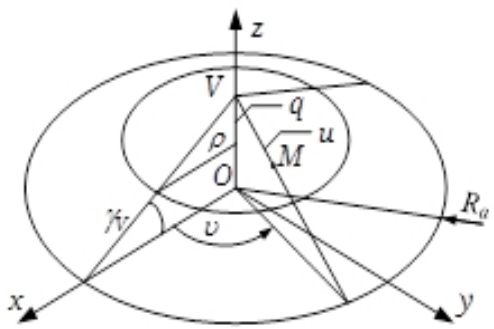

Figure 2. *The parametrization of the conical surface*

circle, and v is the polar angle. In this case the following equations result:

$$\begin{aligned} x_s(\rho,\upsilon) &= \rho\cos\upsilon \\ y_s(\rho,\upsilon) &= \rho\sin\upsilon \\ z_s(\rho,v) &= (R_a-\rho)\,\mathrm{tg}\,\gamma_V+\delta_H \end{aligned} \qquad (17)$$

Equations (17) can be easily put into an alternative form that results by choosing instead the radius, the distance q between the top V and the plane of the arbitrary circle:

$$\begin{aligned} x_s(q,\upsilon) &= q\,\mathrm{ctg}\,\gamma_V\cos\upsilon \\ y_s(q,\upsilon) &= q\,\mathrm{ctg}\,\gamma_V\sin\upsilon \\ z_s(q,\upsilon) &= R_a tg\gamma_V+\delta_H-q \end{aligned} \qquad (18)$$

Starting from parametric forms (16), (17) and (18) the same implicit equation of the conical rake face results:

$$x_s^2+y_s^2-\left((R_a-\rho)\,\mathrm{tg}\,\gamma_V+\delta_H\right)^2\mathrm{ctg}^2\,\gamma_V=0 \qquad (19)$$

2. The equations of the side edge

The side edge result is the intersection of the tooth flank and the rake face. This consists of two distinct segments:

– the edge segment resulting from the involute helix surface;
– the edge segment resulting from the dedendum transition surface.

The length of the second segment grows up significantly near the limit of undercut. It is well known that in this case it puts in shadow the corresponding involute segment, thus it will trim the addendum of the cut tooth at a given height. This phenomenon is not analyzed in the present paper.

2.1. The use of the parametric equations of the cone

Let us consider parametric equations (8) and (16). the dependence between the parameters will be obtained by equating the correspondent coordinate functions:

$$\begin{aligned} x_s(\varphi,v) &= x_s(u,\upsilon) \qquad (a) \\ y_s(\varphi,v) &= y_s(u,\upsilon) \qquad (b) \\ z_s(\varphi,v) &= z_s(u,\upsilon) \qquad (c) \end{aligned} \qquad (20)$$

Applying the following transformations, a system of equations equivalent with (20) results:

$$\begin{aligned} (a') &\leftarrow (a)^2+(b)^2 \\ (b') &\leftarrow (b)/(a) \\ (c') &\leftarrow (c) \end{aligned} \qquad (21)$$

The equivalent system after computing becomes:

$$\begin{aligned} R_b^2\left(1+v^2\right) &= u^2\cos^2\gamma_V \\ \upsilon &= \varphi-\eta-\mathrm{arctg}\,v \\ p\varphi-pv &= R_a\,\mathrm{tg}\,\gamma_V+\delta_H u\sin^2\gamma_V \end{aligned} \qquad (22)$$

This leads to the relation between the independent parameters of the conical surface:

$$\upsilon(u)=\left(R_a\,\mathrm{tg}\,\gamma_V+\delta_H-u\sin\gamma_V\right)p^{-1}-\eta+ +\mathrm{inv}\left(\mathrm{arctg}\sqrt{\frac{u^2\cos^2\gamma_V}{R_b^2}-1}\right) \qquad (23)$$

The second variant of the dependence between the parameters of the conical surface can be obtained from equations (8) and (17). In the same way relations (21) will be applied. After the calculus results the following, simpler form:

$$\upsilon(\rho)=\frac{(R_a-\rho)\,\mathrm{tg}\,\gamma_V+\delta_H}{p}-\eta+ +\mathrm{inv}\left(\mathrm{arctg}\sqrt{\frac{\rho^2}{R_b^2}1}\right) \qquad (24)$$

Functions (23) and (24) equivalent. This is easy to prove by applying the substitution $\rho=u\cos\gamma_V$ to function (23).

The dependence between the parameters of the involute helix results from equations (8) and (19). It results:

$$\varphi(v)=\frac{R_a\,\mathrm{tg}\,\gamma_V+\delta_H}{p}+v\frac{R_b}{p}\,\mathrm{tg}\,\gamma_V\sqrt{1+v^2} \qquad (25)$$

3. The precision of the edge coordinates

Considering the dependences between the independent surface-parameters presented above, the edge point's coordinates can be computed in two ways:

– by substitution in the parametric equations of the cone;
– using the parametric equations of the involute helix.

The precision is defined through the computational error when substituting the coordinates in the implicit surface functions.

The implicit form of the involute helix that results from parametric form (8) becomes:

$$G(x,y,z):\frac{y}{x}-\operatorname{tg}\left(\frac{z}{p}-\eta+\sqrt{\frac{x^2+y^2}{R_b^2}-1}\right)- \quad (26)$$

$$\operatorname{arctg}\sqrt{\frac{x^2+y^2}{R_b^2}-1}=0$$

The numerical evaluation was performed considering a shaper cutter having z_s=21 teeth, module m_n=5 mm and reference rack pressure angle α_0=20°. The top rack angle is set on γ_V=5° with the top relief angle at α_V=6°. (in conformity with JIS-B-1705-1973) and a topland width of s_a= 1,3 mm, the specific profile shift becomes ξ_1=+0,235.

3.1. The errors computed with the function between the parameters of the conical surface

Here the edge coordinates that result from the conical surface are analyzed. That requires the substitution of function (23) in the parametric equations (16). A number of N=30 edge points are considered.

Substituting the computed coordinate values in the implicit equation of the cone leads to the repartition of errors shown in **Figure 3.**

If the same set of coordinates are substituted in the equations of the helical involute, this surprisingly results in significantly smaller error values (**Figure 4.**).

3.2. The errors computed with the function between the parameters of the involute helix surface

In this case edge coordinates are obtained by substituting the dependence (25) in the parametric functions (8). The set of coordinates will be substituted in implicit functions (19) and (26). The repartition of the errors is shown in **Figures 5.** respectively **6.**

By comparison of this figures it can be observed that the errors related to the conical surface present a sort of periodicity while those resulting from the involute helix have a cloud-wise repartition.

4. Conclusions

Performing a simultaneous inspection of repartition graphics presented in the **Figures 3.-6.** allows us to state several conclusions as follows:

The edge coordinates resulting from the conical surface satisfy the implicit equation of this with a maximal error that is 100 times smaller than the errors encountered by the substituting of the

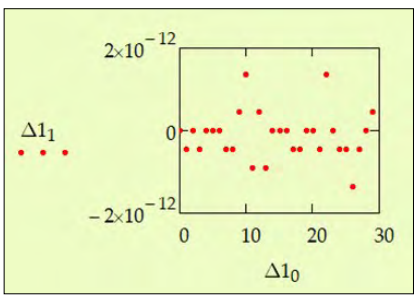

Figure 3. *The repartition of errors related to the conical surface*

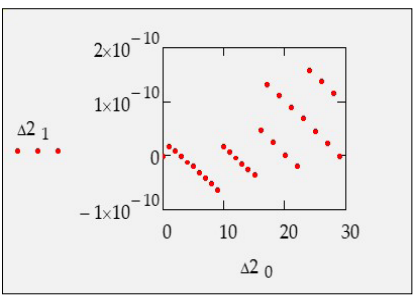

Figure 5. *The repartition of errors related to the conical surface*

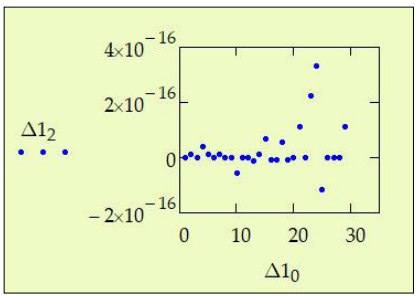

Figure 4. *The repartition of errors related to the involute helix surface*

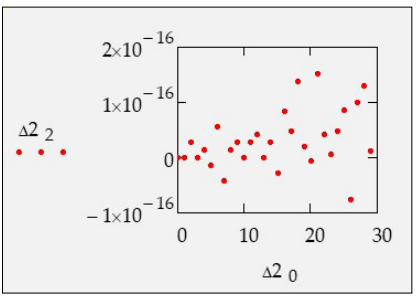

Figure 6. *The repartition of errors related to the involute helix surface*

same coordinates in the implicit equation of the involute helix.

The implicit equation of the helical involute surface is satisfied by the two sets of the edge coordinates at the same precision.

The edge functions derived from the conical surface are much simpler, leading to generating surface functions of lower complexity.

The conclusions are only of theoretical importance while the maximum value of the error is 10E9 times smaller than the narrowest manufacturing tolerance field.

Acknowledgements

The present paper was supported by the Domus- personal research program 4038/24/2018/HTMT.

References

[1] Radzevich P. S.: D*udley's Handbook of Practical Gear Design.* CRC-Press, London, 2016, 368–379.

[2] Radzevich P. S.: *Gear Cutting Tools. Fundamentals of design and computation*, CRC-Press, London, 2010.

[3] Hollanda D.: *Așchiere și scule*. Reprografia I.I.S. Tg. Mureș, 1994. 234–240.

[4] Máté M.: *Hengeres fogaskerekek gyártószerszámai*. Erdélyi Múzeum-Egyesület, Kolozsvár, 2016. 133–158.

[5] Szeniczei L.: *Az általános fogazás*. Nehézipari Műszaki Könyvkiadó, Budapest, 1958. 49–50.

[6] Dudiță Fl., Diaconescu D.: *Mecanisme. Fascicula 2*. Reprografia Universității din Brașov, 1983.

[7] Dudás I.: *The Theory and Practice of Gear Worm Drives*. Penton Press, London, 2000.

[8] Gyenge Cs.: *Lefejtőmarók oldalhátszögének pontos meghatározása és optimálása*. Gép, 48/10. (1996) 38–40.

[9] Máté M., Kántor A. E., Laczkó-Benedek B.: *Metszőkerékkel lefejtett fogaskerekek profilpontosságának vizsgálata*. In: XII. FMTÜ Nemzetközi Tudományos Konferencia kiadványa. Kolozsvár, Románia, Műszaki Tudományos Közlemények 7. 279–283. https://eda.eme.ro/handle/10598/29833.

[10] Tolvaly-Roșca F., Máté M., Forgó Z., Kakucs A.: D*evelopment of Helical Teethed Involute Gear Meshed with a Multi-Edge Cutting Tool Using a Mixed Gear Teeth Modeling Method*. Procedia Engineering 181. (2017) 153–158. https://doi.org/10.1016/j.proeng.2017.02.421